IEEE Access
Multidisciplinary ⋮ Rapid Review ⋮ Open Access Journal

Received 27 March 2023, accepted 9 April 2023, date of publication 20 April 2023, date of current version 1 May 2023.

Digital Object Identifier 10.1109/ACCESS.2023.3268711

RESEARCH ARTICLE

Digital Twin-Driven Fault Diagnosis for Autonomous Surface Vehicles

RAVITEJ BHAGAVATHI[1], D. KWAME MINDE KUFOALOR[2], AND AGUS HASAN[3], (Senior Member, IEEE)
[1]Offshore Simulator Centre AS, 6009 Ålesund, Norway
[2]Maritime Robotics AS, 7010 Trondheim, Norway
[3]Department of ICT and Natural Sciences, Norwegian University of Science and Technology (NTNU), 6009 Ålesund, Norway

Corresponding author: Agus Hasan (agus.hasan@ntnu.no)

This work was supported in part by Equinor ASA.

ABSTRACT This paper presents a digital twin-driven fault diagnosis approach based on a graphical model and an adaptive extended Kalman filter algorithm for autonomous surface vehicles. In contrast with the traditional adaptive Kalman filter algorithm, where the fault parameters are treated as extended state variables, the newly proposed adaptive extended Kalman filter algorithm estimates the magnitude of the faults by calculating the parameter estimation gains directly from the sensor systems. To this end, the algorithm utilizes data from a global navigation satellite system receiver assuming the persistence of excitation conditions on the control inputs. The algorithm is tested in the Otter, an autonomous surface vehicle developed by Maritime Robotics, in which one of its propellers is faulty. Technically, the digital twin receives real-time data from the sensor system, estimates the magnitude of the actuator faults, and visualizes the results in a web-based application using JavaScript with Three.js library and Mapbox for real-world 3D map generation. Information regarding the magnitude of the faults is important for fault-tolerant control. Simulation and experimental results show the proposed approach is able to detect and estimate the actuator faults accurately.

INDEX TERMS Digital twin, fault diagnosis, autonomous systems.

I. INTRODUCTION

The use of models, both physical and digital, has been central in various fields of science, engineering, and technology [1]. Ever since computers came into existence, system modeling has also been digitized and the applications have grown multifold. For example, computer-aided design (CAD) programs make it easier to create and animate visual geometric models and computer-aided engineering (CAE) software runs complex simulations based on numerical models [2]. These digital tools enable their users to fully harness the power of modeling and simulation in the design and analysis of a wide range of physical systems and processes. For example, finite-element modeling and simulation help in the design of safer bridges and buildings [3], while computational fluid dynamic simulations are vital in the aerodynamic and hydrodynamic analysis of fuel-efficient aircraft and ships [4], respectively.

Though it is needless to stress the importance of modeling and simulation in the design stage, their usage does not progress into the operational stage. This is due to the inherent simplifications made in the model which can no longer be valid due to changing system parameters and complex interactions with the environment. Therefore, more advanced digital tools are needed to represent the system through its entire life cycle. Digital twinning is a recent technological trend in engineering that can bridge the gap and provide a platform for continuous interface with a system throughout its life cycle. Together with other emerging technologies such as Cloud Computing, the Internet of Things (IoT), Artificial Intelligence (AI), and Machine Learning (ML), digital twins are expected to play a huge role in Industry 4.0 [5]. Unlike traditional models, which are of limited use during service, digital twins incorporate dynamic

The associate editor coordinating the review of this manuscript and approving it for publication was Baoping Cai.

FIGURE 1. **The Otter ASV used in the experiment is fitted with two fixed propellers.**

system models which are effective, especially during system operation.

A. MOTIVATION

This paper is motivated by an actuator fault diagnosis problem encountered in autonomous surface vehicles (ASV). An ASV is a special class of autonomous mobile systems that perform a wide variety of tasks in challenging environments without any human intervention [6]. Owing to their advanced instrumentation and autonomy, these vehicles have various research and military applications such as seabed mapping, harbor security, ocean environmental monitoring, search and rescue, and reconnaissance. In this paper, we consider an ASV shown in Figure 1. The vehicle is called the Otter and is developed by Maritime Robotics.

The Otter ASV has two fixed propellers mounted at the rear end of the vehicle. The vehicle is under-actuated since it has fewer actuators than its degrees of freedom. To move the ASV forward, each of these propellers needs to produce the same thrust. Otherwise, different thrusts can be applied to maneuver the ASV either to the left or right. The actuator system of the ASV is prone to faults. Common problems include a broken propeller due to an impact with the seabed and a fishing line getting caught in the propeller. This causes a decrease in the performance of the actuator system. Thus, there is an incentive to diagnose the faults as soon as possible before the ASV becomes uncontrollable. In this case, the digital twin is used for actuator fault diagnosis, i.e., to detect and estimate the magnitude of the actuator fault of the Otter ASV in real time.

B. LITERATURE REVIEW

Digital twins in the maritime sector are not new. For example, in 2021 Major et al. [7] created a real-time digital twin of the research vehicle RV Gunnerus and used the twin for condition monitoring of the ship and onboard crane system. Furthermore, Alexander Danielsen-Haces [8] has documented the development of a digital twin platform for different autonomous ship models. In his work, a fault detection feature for ship thruster faults is implemented using machine learning along with the necessary digital twin infrastructure. Up until now, most of the literature on digital twins are focused on predictive maintenance and condition monitoring applications. Predictive maintenance is more relevant in high-value assets with continuous operation, where downtime leads to significant costs. In the context of ASV, given the complex nature of the environment in which they operate with minimum human supervision, condition monitoring is deemed to be more useful.

Fault diagnosis can be found in many pieces of literature and has been implemented for many applications, e.g., subsea blowout preventer [9], and hydraulic control system [10]. In 2018, Zhang [11] proposed an adaptive Kalman filter (AKF) algorithm to monitor the actuator fault of Linear Time Variant/Linear Parameter Varying (LTV/LPV) systems. Extending this work for non-linear systems, Skriver et al. [12] developed an adaptive extended Kalman filter (AEKF) algorithm for actuator fault diagnosis and tested the method in simulations. In another work, Alessandri et al. [13] applied a fault diagnostic system based on a bank of EKF fault estimators for an unmanned underwater vehicle (UUV) in simulations. Furthermore, Ko et al. [14] used a two-stage EKF filter to estimate sensor and actuator faults in which real experimental data is used for IMU sensor faults, while simulated data is used for thruster faults due to difficulties in introducing thruster faults in experiments. They achieve satisfactory results for sensor fault estimation; however, they notice a time delay in thruster fault estimation. Subsequently, Zhou et al. [15] used a fault and state observer in the case of unmanned surface vehicles (USV) in network environments. They also implemented a fault-tolerant control system based on the observer estimates in a simulated environment. Moreover, Abed et al. [16] implemented a Neural Network for fault diagnosis of USV trolling motors trained on the data from the stator current and motor vibrations. Another interesting application of digital twins for USV is the system identification of hydrodynamic parameters using machine learning [17] and model-based methods [18]. In recent work, Kapteyn et al. [19] proposed a mathematical framework for developing digital twins at scale. The framework is based on probabilistic graphical models, which inherently support representation and inference making them best suitable for digital twin applications. It is one of the few works, which attempts to define a mathematical model for digital twins.

Based on the above review, it is noted that the digital twin development for autonomous vehicles still lacks standardization. Thus, there is an incentive to create a standardized framework that can be used for different applications. In this case, our approach is to use a graphical model combined with an AEKF algorithm. Furthermore, most model-based algorithms developed in the previous studies have been tested only in computer simulations. Implementation in a real platform may not be trivial and produce slightly different results and thus need to be studied and experimentally tested.

C. CONTRIBUTION OF THIS PAPER

The contributions of this paper are two-fold:

- A novel framework for digital twin-driven fault diagnosis based on the graphical model and AEKF algorithm that can be used for condition monitoring of ASV actuator systems. The framework can be extended to develop other digital twin features, such as predictive maintenance, remote monitoring, and system optimization for autonomous systems.
- Development and validation of an AEKF algorithm for actuator fault diagnosis of an ASV in real experiments. While the method has been previously proven to be robust in simulated and fictive problems, this is the first time it has been successfully applied to an actual autonomous platform. This achievement is significant, as it demonstrates the effectiveness and practicality of digital twin-driven fault diagnosis in real-world scenarios. The successful application provides evidence of its reliability and accuracy in detecting actuator faults.

II. THEORETICAL BACKGROUND

Hybrid modeling techniques which combine physics-based and data-driven methods while utilizing the data from the real system are better suitable for a wide range of digital twin applications. Probabilistic graphical models, particularly dynamic Bayesian networks, are one such class of hybrid modeling methods that are found to adequately address the needs of digital twin models at scale [19]. It is reasonable to state that systems that warrant digital twin representations usually also contain inherent *complexity* and *uncertainty*. If the system is simple and deterministic, a dynamic model of the system will be able to represent it at all times. However, that is not the case with most real-world systems. At least, the ones that are the subject of this work. Complexity in systems arises from multiple factors. In engineering systems, they can arise from structural complexity due to a large number of interacting subsystems, parts, and components and their relationships. Complexity can also arise from system dynamics due to the time-varying nature of system states and parameters. This is called dynamic complexity. Uncertainty, like complexity, is inherent in most real-world systems models both because of abstractions and assumptions made while modeling the system and also because of the noisy observations that are used to update these models [20]. Owing to the dual challenge posed by *complexity* and *uncertainty*, a robust hybrid modeling framework is required to incorporate physics-based and/or data-driven methods along with the knowledge transferred from the real system via data while handling the system uncertainty and complexity. The graphical model uses a graph-based representation to encode a complex relation of variables over a high-dimensional space. They combine graph theory with estimation theory and are shown to facilitate *representation*, *inference*, and *learning*, which are the cornerstones of complex system modeling. *Representation* is the encoding of knowledge about the system in a machine-readable format, *inference* is the ability to use the existing representation to perform meaningful analysis of the system

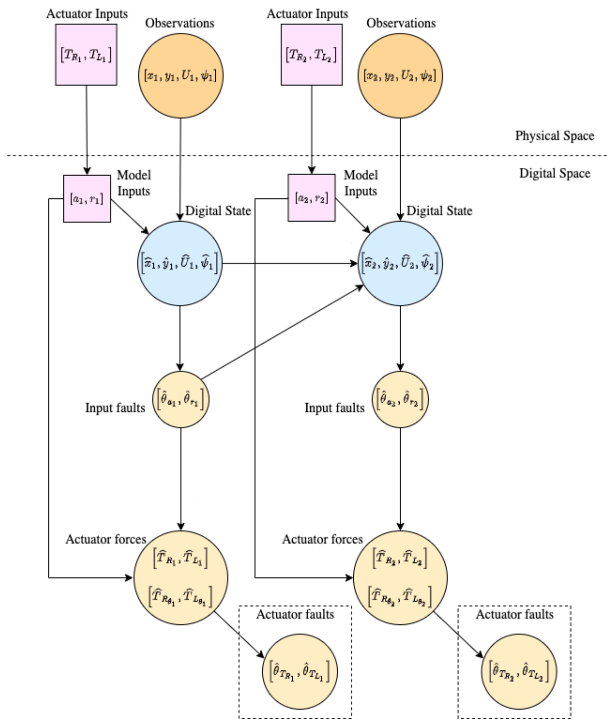

FIGURE 2. A digital twin framework for actuator fault diagnosis based on a graphical model and AEKF.

and *learning* is the ability to use past experience and data to update the existing representation [21].

Inspired by the recent work on the probabilistic graphical models presented in [19], in this paper, we propose a novel approach for fault diagnosis of ASVs by utilizing a graphical model combined with an AEKF algorithm, as illustrated in Figure 2. The proposed approach leverages information from the physical system to extract hidden information in the digital space. The digital space refers to the virtual representation of a physical system that allows us to test and validate various scenarios and changes to the physical system. By leveraging the digital space in digital twin technology, we can improve operational efficiency, reduce maintenance costs, and increase the asset lifespan of the ASVs. The digital model in the digital space simulates the behavior and characteristics of the physical entity in real-time or near real-time. This digital space can include various types of data such as design specifications, sensor readings, operational data, maintenance records, and other relevant information. To map the physical system into the digital space, we define state variables such as x_i, y_i, U_i, and ψ_i, which represent the position in the x-axis, position in the y-axis, forward velocity, and course angle of the ASV at time step i, respectively. These state variables can be measured from various sensor systems, such as the global navigation satellite system (GNSS), Inertial Measurement Unit (IMU), or Simultaneous Localisation and Mapping (SLAM). In Section IV, we propose and implement an AEKF algorithm to estimate the fault parameters θ_α and θ_r associated with faults in the actuator systems, which affected the acceleration and course angle. We denote $\hat{x}_i$, $\hat{y}_i$, $\hat{U}_i$, $\hat{\psi}_i$, $\hat{\theta}_\alpha$, and $\hat{\theta}_r$ as the variables and parameters in the digital space. These estimated variables and parameters are needed to calculate the propeller thrust $\hat{T}_R$ and $\hat{T}_L$, which are used to estimate the propeller faults $\hat{\theta}_{T_R}$, and $\hat{\theta}_{T_L}$. The update equation in the AEKF is derived from a simple nonlinear dynamic model of an ASV presented in Section III. It is worth noting that, in contrast with the traditional AEKF algorithm, where the fault parameters θ_α and θ_r are considered as additional state variables, the AEKF algorithm developed in this paper estimates the parameters directly from sensor measurements. This method allows for more efficient and accurate fault diagnosis in ASVs.

III. SYSTEM MODELING

A. DYNAMIC MODEL OF THE ASV

The generic continuous-time dynamic model of the Otter ASV can be written as:

$$\dot{x}(t) = U(t)\cos(\psi(t)) \tag{1}$$
$$\dot{y}(t) = U(t)\sin(\psi(t)) \tag{2}$$
$$\dot{U}(t) = a(t) \tag{3}$$
$$\dot{\psi}(t) = r(t) \tag{4}$$

where x and y are the positions in the North-East coordinate, U is the forward speed, and ψ is the course angle. In this model, the linear acceleration a and the course rate r are considered as control inputs and can be estimated using different sensor systems such as an inertial measurement unit (IMU), an encoder, or a GNSS receiver. If the latter is used, the estimates need to be filtered to avoid rapid changes as follows:

$$\dot{a}(t) = \frac{1}{\tau_a}\left(\mathrm{sat}(a_c(t)) - a(t)\right) \tag{5}$$
$$\dot{r}(t) = \frac{1}{\tau_r}\left(\mathrm{sat}(r_c(t)) - r(t)\right) \tag{6}$$

where a_c and r_c are determined from a backward finite difference approximation:

$$a_{c,m} = \frac{(1-\alpha)U_m^{GNSS} + \alpha U_{m-1}^{GNSS} - U_{m-2}^{GNSS}}{(1-\alpha)\Delta_1 + \Delta_2} \tag{7}$$
$$r_{c,m} = \frac{(1-\alpha)\psi_m^{GNSS} + \alpha \psi_{m-1}^{GNSS} - \psi_{m-2}^{GNSS}}{(1-\alpha)\Delta_1 + \Delta_2} \tag{8}$$

where $\alpha = \frac{(\Delta_1+\Delta_2)^2}{\Delta_1^2}$. The symbol "sat" refers to the saturation function. Here, τ_a and τ_r are the user-defined time constants, while Δ_1 and Δ_2 are the time steps. Let $\boldsymbol{x} = \begin{pmatrix} x & y & U & \psi \end{pmatrix}^\intercal$ denotes the state variable of the ASV. Applying the Euler's method to (1)-(4), we have:

$$\boldsymbol{x}_{k+1} = \boldsymbol{f}(\boldsymbol{x}_k) + \boldsymbol{B}\boldsymbol{u}_k \tag{9}$$

where

$$\boldsymbol{f}(\boldsymbol{x}_k) = \begin{pmatrix} x_k + \Delta t U_k \cos(\psi_k) \\ y_k + \Delta t U_k \sin(\psi_k) \\ U_k \\ \psi_k \end{pmatrix} \tag{10}$$

$$\boldsymbol{B} = \begin{pmatrix} 0 & 0 \\ 0 & 0 \\ \Delta t & 0 \\ 0 & \Delta t \end{pmatrix}, \quad \boldsymbol{u}_k = \begin{pmatrix} a_k \\ r_k \end{pmatrix} \tag{11}$$

The nonlinear state-space model (9) is only valid if the Otter is in perfect condition and is sailing in ideal weather. In practice, this is not always the case. Thus, we need to model the external disturbance, such as wind, and the internal aspect such as actuator faults. To this end, we add two terms into (9), such that we have:

$$\boldsymbol{x}_{k+1} = \boldsymbol{f}(\boldsymbol{x}_k) + \boldsymbol{B}\boldsymbol{u}_k + \boldsymbol{\Phi}_k\boldsymbol{\theta} + \boldsymbol{w}_k \tag{12}$$

Here, the fault parameter $\boldsymbol{\theta} = \begin{pmatrix} \theta_a & \theta_r \end{pmatrix}^\intercal$ represents the magnitude of the fault caused by a malfunction in the actuator system and is unknown. The function $\boldsymbol{\Phi}_k$ is known and is given by $\boldsymbol{\Phi}_k = -\boldsymbol{B}\mathrm{diag}(\boldsymbol{u}_k)$. The actuator terms in (12) becomes $\boldsymbol{B}\boldsymbol{u}_k - \boldsymbol{B}\mathrm{diag}(\boldsymbol{u}_k)\boldsymbol{\theta} = \boldsymbol{B}(\boldsymbol{I} - \mathrm{diag}(\boldsymbol{\theta}))\boldsymbol{u}_k$. In this case, we can see that the fault $\boldsymbol{\theta}$ enters the system (12) as the actuator loss of effectiveness. The vector $\boldsymbol{w}_k$ describes the wind-induced disturbances. The uncertainty is also appeared in the sensor system, such that the measured data becomes:

$$\boldsymbol{y}_k = \boldsymbol{C}\boldsymbol{x}_k + \boldsymbol{v}_k \tag{13}$$

where the uncertainty $\boldsymbol{v}_k$ is assumed to be white Gaussian noise. Since all state variables can be measured, then $\boldsymbol{C} = \boldsymbol{I}_4$. Remark that the model (1)-(4) is a generic model for a mobile system; thus, the method presented in this paper can be implemented for other mobile robots.

B. DESCRIPTIVE MODEL OF THE ASV

The Otter, as shown in Figure 3, runs on electric propulsion with a total installed power of 1830Wh from two Torqeedo™ batteries and is driven by two Torqeedo Ultralight 403 AC trolling motors which provide a static thrust of 15Kg each. Additionally, it is equipped with a GNSS sensor for navigation and a camera for capturing video feeds. Furthermore, the Otter is powered by a Raspberry Pi as its main computer, also referred to as OBS (On-board System), and an additional Intel-based payload computer running Windows 10 OS for integrating optional payload sensors. There are four channels of communication with the Otter, namely VHF Radio, 4G, WiFi, and Ethernet. This gives a wide range of choices for the users to select a preferred communication channel based on application requirements and range limitations. In total, the Otter weighs 55Kg and has an overall size of 2m x 1m x 0.8m in length, breadth, and height dimensions, respectively. This system description is important to understand the capabilities and limitations of the vehicle before we proceed to develop a specific application for the digital twin.

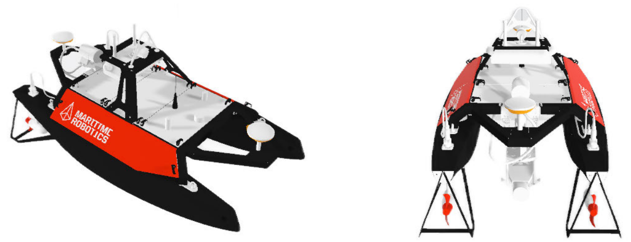

FIGURE 3. 3D CAD model of the Otter ASV.

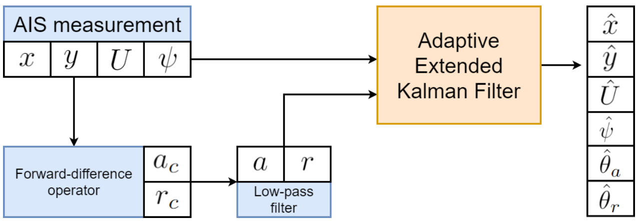

FIGURE 4. Fault diagnosis based on a hybrid approach, which combines physics-based and data-driven.

IV. FAULT DIAGNOSIS ALGORITHM

In this work, we mainly focus on actuator faults. Actuator faults can cause the vehicles to be partially or completely uncontrollable. In this case, if the actuator faults have been diagnosed, the operator can decide whether the mission should be continued or stopped. The key point when diagnosing the fault is prompt detection of process malfunctions in the system [22]. Given the sophisticated nature of today's systems, manual supervision of faults in all the system components is not a feasible solution. Hence, there is an increasing move towards automatic supervision of system abnormalities.

In this paper, we approach the fault diagnosis problem using a hybrid-based method, as presented in Figure 4. Here, measurement data obtained from the GNSS/AIS sensor are combined with the vehicle model in the AEKF algorithm to estimate the fault parameters $\hat{\theta}_a$ and $\hat{\theta}_r$. Extending the work in [11] for linear systems, we linearize the nonlinear system (12) at $\hat{\boldsymbol{x}}_k$. Thus, we have:

$$\boldsymbol{x}_{k+1} = \boldsymbol{F}_k(\hat{\boldsymbol{x}}_k)\boldsymbol{x}_k + \boldsymbol{E}_k(\hat{\boldsymbol{x}}_k) + \boldsymbol{B}\boldsymbol{u}_k + \boldsymbol{\Phi}_k\boldsymbol{\theta} + \boldsymbol{w}_k \tag{14}$$

where $\boldsymbol{F}_k(\hat{\boldsymbol{x}}_k) = \frac{\partial \boldsymbol{f}(\boldsymbol{x}_k,\boldsymbol{y}_k)}{\partial \boldsymbol{x}_k}\Big|_{\hat{\boldsymbol{x}}_k}$, $\boldsymbol{E}_k(\hat{\boldsymbol{x}}_k) = \boldsymbol{f}(\hat{\boldsymbol{x}}_k,\boldsymbol{y}_k) - \frac{\partial \boldsymbol{f}(\boldsymbol{x}_k,\boldsymbol{y}_k)}{\partial \boldsymbol{x}_k}\Big|_{\hat{\boldsymbol{x}}_k}\hat{\boldsymbol{x}}_k$. For simplicity, we define $\boldsymbol{F}_k = \boldsymbol{F}_k(\hat{\boldsymbol{x}}_k)$ and $\boldsymbol{E}_k = \boldsymbol{E}_k(\hat{\boldsymbol{x}}_k)$. The Kalman gain $\boldsymbol{K}_{k+1}$ and the error covariance matrix $\boldsymbol{P}^+_{k+1}$ are computed using the following standard recursion:

$$\boldsymbol{P}^-_{k+1} = \boldsymbol{F}_k\boldsymbol{P}^+_k\boldsymbol{F}^\top_k + \boldsymbol{Q}^F_k \tag{15}$$
$$\boldsymbol{\Sigma}_{k+1} = \boldsymbol{C}\boldsymbol{P}^-_{k+1}\boldsymbol{C}^\top + \boldsymbol{R}^F_k \tag{16}$$
$$\boldsymbol{K}_{k+1} = \boldsymbol{P}^-_{k+1}\boldsymbol{C}^\top\Sigma^{-1}_{k+1} \tag{17}$$
$$\boldsymbol{P}^+_{k+1} = [\boldsymbol{I}_n - \boldsymbol{K}_{k+1}\boldsymbol{C}]\boldsymbol{P}^-_{k+1} \tag{18}$$

while the gains $\boldsymbol{\Pi}_{k+1}$ and $\boldsymbol{\xi}_{k+1}$ are calculated from:

$$\boldsymbol{\xi}_{k+1} = (\boldsymbol{I}_n - \boldsymbol{K}_{k+1}\boldsymbol{C})\boldsymbol{F}_k\boldsymbol{\xi}_k \tag{19}$$
$$+ (\boldsymbol{I}_n - \boldsymbol{K}_{k+1}\boldsymbol{C})\boldsymbol{\Phi}_k \tag{20}$$
$$\boldsymbol{\zeta}_{k+1} = \boldsymbol{C}\boldsymbol{F}_k\boldsymbol{\xi}_k + \boldsymbol{C}\boldsymbol{\Phi}_k \tag{21}$$
$$\Lambda_{k+1} = \left[\lambda\boldsymbol{\Sigma}_{k+1} + \boldsymbol{\zeta}_{k+1}\boldsymbol{S}_k\boldsymbol{\zeta}^\top_{k+1}\right]^{-1} \tag{22}$$
$$\boldsymbol{\Pi}_{k+1} = \boldsymbol{S}_k\boldsymbol{\zeta}^\top_{k+1}\Lambda_{k+1} \tag{23}$$
$$\boldsymbol{S}_{k+1} = \frac{1}{\lambda}\boldsymbol{S}_k - \frac{1}{\lambda}\boldsymbol{S}_k\boldsymbol{\zeta}^\top_{k+1}\Lambda_{k+1}\boldsymbol{\zeta}_{k+1}\boldsymbol{S}_k \tag{24}$$

Finally, the fault and the state are estimated using the following formula:

$$\hat{\boldsymbol{\theta}}_{k+1} = \hat{\boldsymbol{\theta}}_k + \boldsymbol{\Pi}_{k+1}\tilde{y}_k \tag{25}$$
$$\hat{\boldsymbol{x}}_{k+1} = \boldsymbol{A}\hat{\boldsymbol{x}}_k + \boldsymbol{f}(\boldsymbol{x}_k,\boldsymbol{y}_k) + \boldsymbol{B}\boldsymbol{u}_k + \boldsymbol{\Phi}_k\hat{\boldsymbol{\theta}}_k + \boldsymbol{K}_{k+1}\tilde{\boldsymbol{y}}_k + \boldsymbol{\xi}_{k+1}[\hat{\boldsymbol{\theta}}_{k+1} - \hat{\boldsymbol{\theta}}_k] \tag{26}$$

where $\tilde{y}_k = \boldsymbol{y}_k - \boldsymbol{C}\hat{\boldsymbol{x}}_k$. The forgetting factor λ dictates the convergence rate. Bigger λ causes slower transient behavior, and vice versa. The main advantage of using the AEKF algorithm is that the method is applicable for general nonlinearity, once the Jacobian matrix can be computed. Furthermore, the method can handle process and measurement noise. However, due to linearization, the estimates may not converge to the actual values. This limitation can be addressed by adding a nonlinear observer (NLO) to guarantee stability.

V. NUMERICAL SIMULATION AND EXPERIMENTAL RESULTS

A. NUMERICAL SIMULATION

As a simple demonstration of the digital twin-driven fault diagnosis approach, a dynamic model of an autonomous surface vehicle with known actuator faults is used in simulation to generate the state variable data. The generated data is then used by the AEKF algorithm to estimate the state variables and fault parameters. The results of the simulation and estimation are shown in Figure 5. The simulation is run for 20 seconds with a sampling time of 0.0001s. The non-zero control inputs given to exciting the system are the linear acceleration a and course rate r. In this example, the faults are represented by the actuator's loss of effectiveness which affects the control inputs. Both actuator faults occur at $t = 5s$. The first control input losses 50% of the effectiveness, while the second control input losses 30% of the effectiveness. It can be observed that the AEKF estimates the faults accurately in less than 1s. We can further observe that the estimation algorithm is able to follow the changes in the actuator fault accurately. This is a simple demonstration of the fault parameter estimation algorithm in an ideal case with step inputs and step faults. An important parameter that affects the convergence of estimation is the forgetting factor λ. This acts as a tuning parameter with higher values suppressing the noise and resulting in smoother estimates but also slowing down the convergence. A comprehensive paper regarding the comparative performance of the AEKF with other methods has been presented by the last author in the

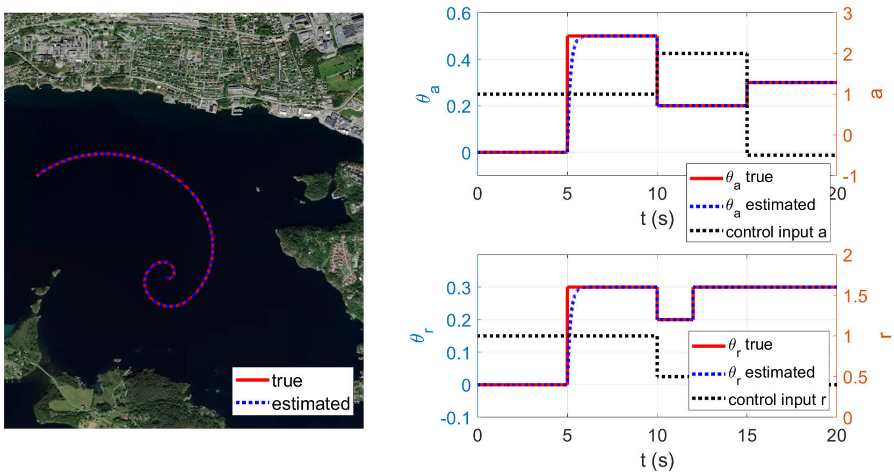

FIGURE 5. **State variable (left) and fault parameter (right) estimation based on the vehicle model (1)–(4) with known faults.**

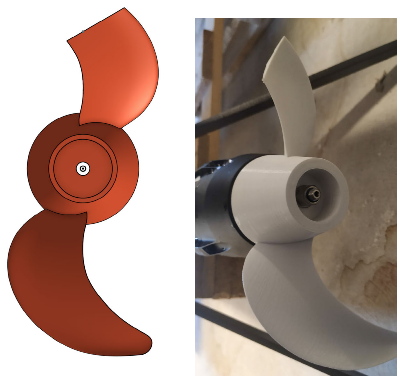

(a) 3D model of the broken propeller (b) The actually broken propeller

FIGURE 6. **One of the Otter propellers is broken to simulate faulty condition.**

following paper [23]. The main advantage of the AEKF is the method can be applied to many nonlinear systems as long as the Jacobian can be calculated.

B. EXPERIMENTAL RESULTS

To demonstrate the digital twin-driven fault diagnosis approach in the actual autonomous surface vehicle platform, real data from the Otter with faulty actuators is needed. The faults can then be estimated using the proposed AEKF algorithm. For this purpose, the Otter is taken to sea trials with two propeller settings. The first setting is to use perfectly working propellers, while the second setting is when one of the propellers is broken. The sea trials were carried out at Sunnmøre Museum dock in Ålesund, Norway. The Otter is operated to track two paths in way-point mode using a vehicle control station (VCS) provided by Maritime Robotics. Path 1 is a straight-line maneuver and Path 2 is an S-manoeuvre. The reason for choosing these different paths is to test the performance of the fault detection algorithm in different scenarios.

A 3D model of the original propeller is created using CAESES®, a propeller design software from Friendship Systems™ and further modified in OnShape™, a cloud-based CAD software. The 3D model is made with the help of visual reference from the original propeller. Therefore, it is not precisely similar to the original propeller. However, this difference will either not matter due to the robust closed-loop control system of the Otter or it will be picked up as a fault by the fault diagnosis algorithm. The 3D model is further modified by creating a broken blade to simulate a faulty propeller. Both the 3D models, intact and broken, are then 3D printed on Prusa MK3S ® 3D printers.

For implementing the actuator fault diagnosis algorithm on the above system, it should satisfy the completely observable and completely controllable condition. For this purpose, we need state observations $\begin{pmatrix} x & y & U & \psi \end{pmatrix}^\mathsf{T}$ from the Otter. The Otter is equipped with a GNSS sensor which logs the location, orientation, and speed as latitude, longitude, speed-over-ground (SOG), and course-over-ground (COG) in the world frame which can be converted into $\begin{pmatrix} x & y & U & \psi \end{pmatrix}^\mathsf{T}$ in North-East frame. The World Geodetic System (WGS-84) is used to map the latitude and longitude into the Cartesian coordinate. For this purpose, let us define $\Delta l = l - l_0$ and $\Delta \mu = \mu - \mu_0$, where l_0 and μ_0 are the longitude and latitude of the flat Earth coordinate origin. The North and East position (x, y) are computed as:

$$x = \frac{\Delta \mu}{\text{atan2}(1, R_M)} \tag{27}$$

$$y = \frac{\Delta l}{\text{atan2}(1, R_N \cos(\mu_0))} \tag{28}$$

where $R_N = \frac{D_E}{\sqrt{1-e_e^2 \sin^2(\mu_0)}}$ and $R_M = \frac{D_E(1-e_e^2)}{1-e_e^2 \sin^2(\mu_0)}$. Here, D_E is the Earth's equatorial radius and e_e is the Earth's eccentricity.

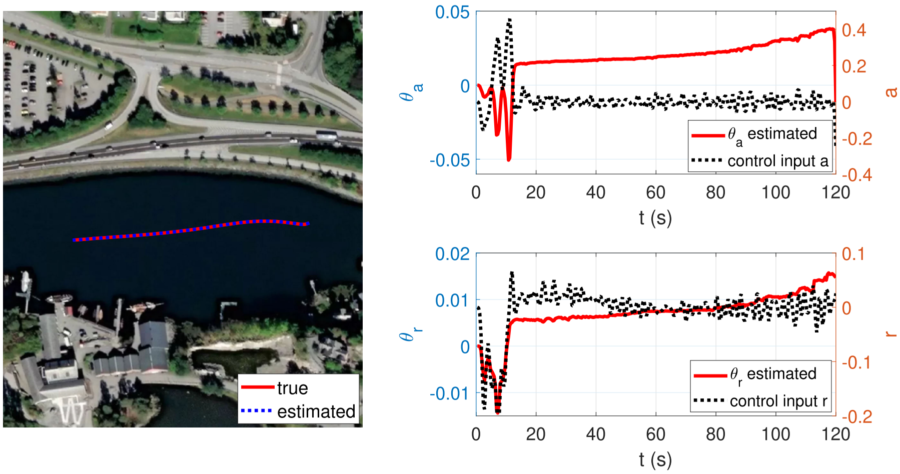

FIGURE 7. Straight-line maneuver (left) and fault estimation with perfectly working propellers (right).

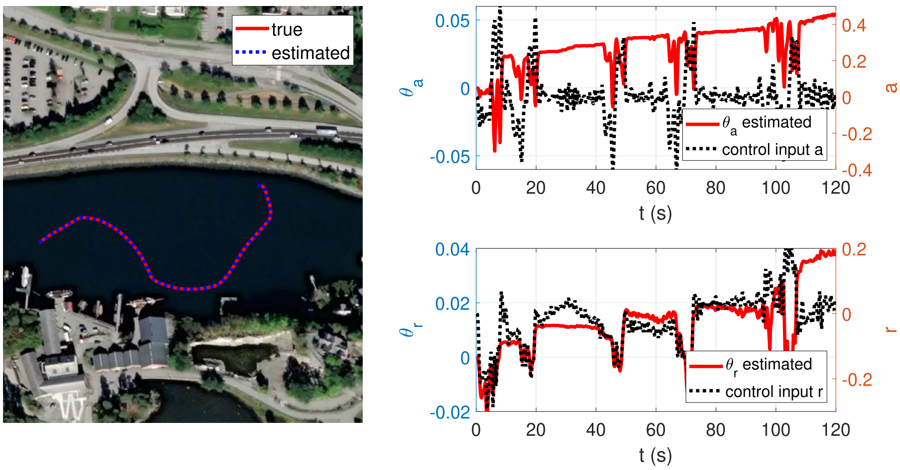

FIGURE 8. S-manoeuvre (left) and fault estimation with perfectly working propellers (right).

1) FAULT-FREE SCENARIO

Figure 7 and Figure 8 show the position and fault parameter estimates for both the maneuvers without faults. From the plots, we can make an observation regarding the faults. The fault estimation is different for both cases though the propeller conditions are the same. Particularly, the estimated value for the S-manoeuvre is higher compared to the straight-line maneuver. However, in both cases, the maximum fault is about 4%. This can be attributed to unknown faulty conditions of the Otter actuator system and the noise in the sensor measurement. At first, these results may seem a bit strange. However, we know that the AEKF algorithm performs fault estimation only with non-zero input. In the case of a straight-line maneuver in Figure 7, the inputs i.e., the acceleration and course rate are close to zero as the Otter is operating in a way-point mode, where it tracks the input trajectory with constant speed. This is the reason for a close-to-zero fault estimation seen in Figure 7. Coming to the second observation of the non-zero faults in inputs in Figure 8, it should be noted that this indicates the faults in input acceleration and course rate but not the actual actuator faults.

The actuator fault magnitudes are small with maximum values of 0.045 and 0.04, respectively. However, one interesting result is the appearance of the peaks which coincide with the curvature of the trajectory. In other words, the fault in the starboard side propeller has a maximum value when the vehicle is turning left. Similarly, the port side propeller has a maximum value when the vehicle is turning right. This logically follows from the above discussion that the fault parameter magnitude depends on the input magnitude. Since a right-turning propeller will have higher input to its port side propeller, this fault magnitude is also higher during that maneuver.

2) FAULTY SCENARIO

A fault was introduced in the actuators by breaking the port propeller. The expected outcome was that the actuator fault value for the port propeller alone would show a peak in the

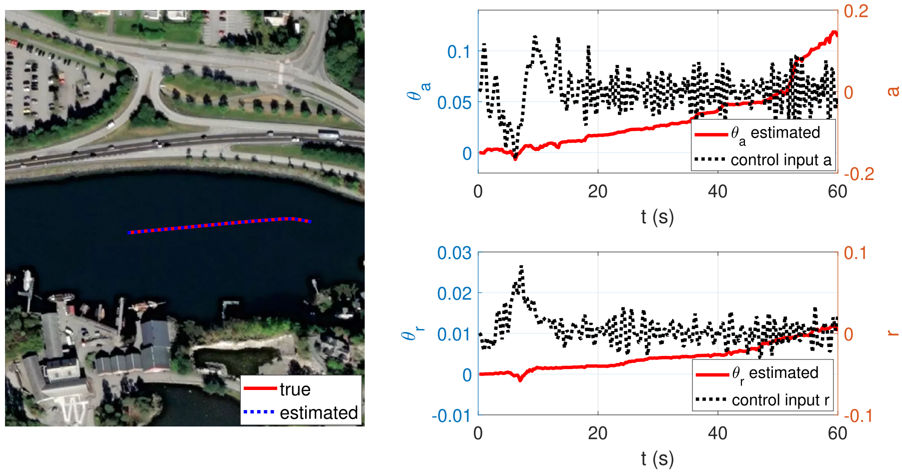

FIGURE 9. Straight-line maneuver (left) and fault estimation with faulty propellers (right).

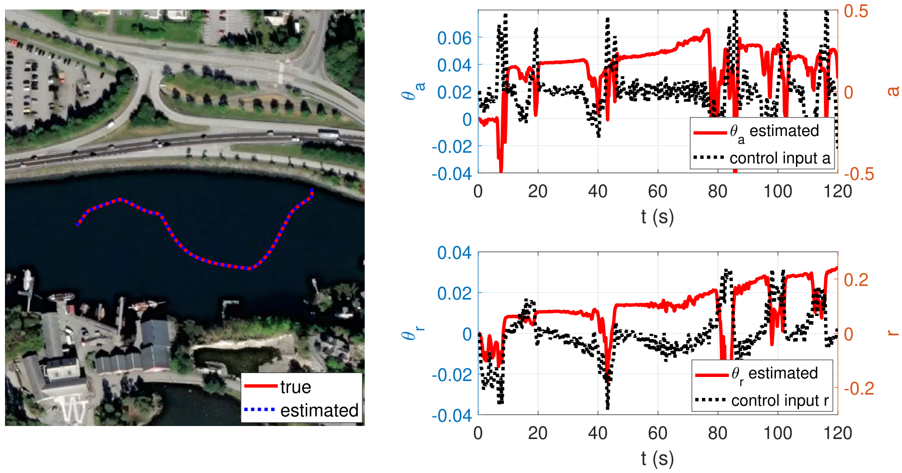

FIGURE 10. S-manoeuvre (left) and fault estimation with faulty propellers (right).

fault curve, while the starboard propeller's fault value would be similar to the earlier tests. As predicted, the fault curve for the port propeller showed a peak with a magnitude of 0.12 (Figure 9), which corresponds to a fault percentage of 12%. This value is significantly higher than the previous cases, where a fault was detected at 4%, and thus validates the AEKF-based fault detection algorithm and the overall fault diagnosis technique. However, it is essential to note that the input fault estimates alone, which are produced by the AEKF, are not sufficient to diagnose a fault. The estimated values are similar for all the test cases. It is through the actuator fault values generated by the dynamic model that we can conclude the presence of the fault, its location, and its magnitude. Figure 10 illustrates the results of the S-shape maneuver, showing that the estimated faults in both the experiment with a broken propeller and the experiment without a broken propeller are identical. This observation can be attributed to the fact that the S-shape maneuver is designed in a way that conceals the presence of faults in the system. Hence, it becomes difficult to detect any faults during the execution of the maneuver. Therefore, the similarity in estimated faults between the two experiments is not an indicator of the absence of a fault, but rather a consequence of the limitations of the maneuver. It is important to note that this does not necessarily mean that there are no faults in the system, and further investigation using other maneuvers or techniques may be necessary to confirm the presence or absence of any faults.

VI. CONCLUSION AND FUTURE WORKS

We have demonstrated a digital twin-driven fault diagnosis approach for an ASV in real-world settings. The demonstration shows the potential benefits of the digital twin technology to increase the safety and reliability of an ASV by monitoring the unknown parameters associated with the health status of the system. The method is based on a graphical method combined with an AEKF algorithm for state and parameter estimation developed previously by the last author. We note that the algorithm may not be working if the nonlinearity of the system is severe. Further works include developing a more robust algorithm for state and parameter estimation. A possible approach is to add a nonlinear observer (NLO) into the estimation method.

REFERENCES

[1] D. Buede and W. Miller, *The Engineering Design of Systems: Models and Methods*. Hoboken, NJ, USA: Wiley, 2016.

[2] P. Kyratsis, K. Kakoulis, and A. P. Markopoulos, ''Advances in CAD/CAM/CAE technologies,'' *Machines*, vol. 8, p. 13, Mar. 2020.

[3] D. Curto, V. Franzitta, A. Guercio, and P. Martorana, ''FEM analysis: A review of the most common thermal bridges and their mitigation,'' *Energies*, vol. 15, no. 7, p. 2318, 2022.

[4] J. Abinesh and J. Arunkumar, ''CFD analysis of aerodynamic drag reduction and improve fuel economy,'' *Int. J. Mech. Eng. Robot. Res.*, vol. 3, no. 4, pp. 430–440, 2014.

[5] T. H.-J. Uhlemann, C. Lehmann, and R. Steinhilper, ''The digital twin: Realizing the cyber-physical production system for Industry 4.0,'' *Proc. CIRP*, vol. 61, pp. 335–340, Jan. 2017.

[6] Z. Liu, Y. Zhang, X. Yu, and C. Yuan, ''Unmanned surface vehicles: An overview of developments and challenges,'' *Annu. Rev. Control*, vol. 41, pp. 71–93, Jan. 2016.

[7] P. Y. Major, G. Li, H. Zhang, and H. P. Hildre, ''Real-time digital twin of research vessel for remote monitoring,'' in *Proc. 35th Eur. Council Modeling Simulation*, 2021, pp. 1–6.

[8] A. Danielsen-Haces, ''Digital twin development, condition monitoring and simulation comparison for the revolt autonomous model ship,'' M.S. thesis, Dept. Eng. Cybern., Norwegian Univ. Sci. Technol., Trondheim, Norway, 2018.

[9] X. Kong, B. Cai, Y. Liu, H. Zhu, C. Yang, C. Gao, Y. Liu, Z. Liu, and R. Ji, ''Fault diagnosis methodology of redundant closed-loop feedback control systems: Subsea blowout preventer system as a case study,'' *IEEE Trans. Syst., Man, Cybern. Syst.*, vol. 53, no. 3, pp. 1618–1629, Mar. 2023.

[10] X. Kong, B. Cai, Y. Liu, H. Zhu, Y. Liu, H. Shao, C. Yang, H. Li, and T. Mo, ''Optimal sensor placement methodology of hydraulic control system for fault diagnosis,'' *Mech. Syst. Signal Process.*, vol. 174, Jul. 2022, Art. no. 109069.

[11] Q. Zhang, ''Adaptive Kalman filter for actuator fault diagnosis,'' *Automatica*, vol. 93, pp. 333–342, Jul. 2018.

[12] M. Skriver, J. Helck, and A. Hasan, ''Adaptive extended Kalman filter for actuator fault diagnosis,'' in *Proc. 4th Int. Conf. Syst. Rel. Saf. (ICSRS)*, Nov. 2019, pp. 339–344.

[13] A. Alessandri, M. Caccia, and G. Veruggio, ''Fault detection of actuator faults in unmanned underwater vehicles,'' *Control Eng. Pract.*, vol. 7, no. 3, pp. 357–368, Mar. 1999.

[14] N. Y. Ko, G. Song, H. T. Choi, and J. Sur, ''Fault detection and diagnosis of sensors and actuators for unmanned surface vehicles,'' in *Proc. 21st Int. Conf. Control, Autom. Syst. (ICCAS)*, Oct. 2021, pp. 1451–1453.

[15] Z. Zhou, M. Zhong, and Y. Wang, ''Fault diagnosis observer and fault-tolerant control design for unmanned surface vehicles in network environments,'' *IEEE Access*, vol. 7, pp. 173694–173702, 2019.

[16] W. Abed, S. Sharma, and R. Sutton, ''Neural network fault diagnosis of a trolling motor based on feature reduction techniques for an unmanned surface vehicle,'' *Proc. Inst. Mech. Eng., I, J. Syst. Control Eng.*, vol. 229, no. 8, pp. 738–750, Sep. 2015.

[17] J. Luo, Y. Shi, and L. Xie, ''An unsupervised learning based simplification on ship motion model and its verification,'' in *Proc. 34rd Youth Academic Annu. Conf. Chin. Assoc. Autom. (YAC)*, Jun. 2019, pp. 52–57.

[18] H. A. U. Sasaki, A. S. S. Ianagui, P. C. de Mello, and E. A. Tannuri, ''Digital twin of a maneuvering ship: Real-time estimation of derivatives and resistance coefficient based on motion sensor,'' in *Proc. Int. Conf. Offshore Mech. Arctic Eng.*, vol. 85161, Oct. 2021, Art. no. V006T06A021.

[19] M. G. Kapteyn, J. V. R. Pretorius, and K. E. Willcox, ''A probabilistic graphical model foundation for enabling predictive digital twins at scale,'' *Nature Comput. Sci.*, vol. 1, no. 5, pp. 337–347, May 2021.

[20] D. Koller and N. Friedman, *Probabilistic Graphical Models: Principles and Techniques*. Cambridge, MA, USA: MIT Press, 2009.

[21] K. Murphy, ''An introduction to graphical models,'' Dept. Comput. Sci., Univ. British Columbia, Vancouver, BC, Canada, Tech. Rep. 96, pp. 1–19, 2001.

[22] R. J. Patton, P. M. Frank, and R. N. Clark, *Issues of Fault Diagnosis for Dynamic Systems*. Berlin, Germany: Springer, 2013.

[23] A. Hasan, M. Tahavori, and H. S. Midtiby, ''Model-based fault diagnosis algorithms for robotic systems,'' *IEEE Access*, vol. 11, pp. 2250–2258, 2023.

RAVITEJ BHAGAVATHI received the B.Tech. degree in naval architecture and ocean engineering from the Indian Institute of Technology Madras, India, and the M.Sc. degree in simulation and visualization from the Norwegian University of Science and Technology (NTNU). He is currently a Software Developer with the Virtual Prototyping Team, Offshore Simulator Centre AS, Ålesund, Norway. His research interests include digital twins and the simulation of cyber-physical systems.

D. KWAME MINDE KUFOALOR received the B.Sc. degree in automation engineering and the M.Sc. and Ph.D. degrees in engineering cybernetics from the Norwegian University of Science and Technology (NTNU). He was a Project Engineer and a Developer of ship power and automation systems with Vard, a Norwegian shipbuilding company. He is currently an Autonomy Architect, an Autonomy Project Manager, and a Situational Awareness Software Team Lead with Maritime Robotics AS. Before joining Maritime Robotics AS, he was a Research Fellow with the Autosea Project, Department of Engineering Cybernetics, NTNU. His research interests include autonomous vehicle guidance, navigation, predictive control, situational awareness, collision avoidance, and fault tolerance.

AGUS HASAN (Senior Member, IEEE) received the B.Sc. degree in mathematics from the Department of Mathematics, Bandung Institute of Technology, and the Ph.D. degree in control systems from the Department of Cybernetics Engineering, Norwegian University of Science and Technology (NTNU). He is currently a Professor of cyber-physical systems with the Department of ICT and Natural Sciences, NTNU. His research interests include cyber-physical systems, system dynamics, digital twins, and autonomous systems. He serves as an IEEE Technical Committee Member on Aerial Robotics and Unmanned Aerial Vehicles and an IFAC Technical Committee Member on Distributed Parameter Systems.